Solid-State NMR Structural Studies of the Ternary Molybdenum Cluster Chalcogenides $Cd_xMo_6Se_8$ ($x = 1, 2$)

Michael Janssen, Hellmut Eckert,* and Werner Müller-Warmuth

Institut für Physikalische Chemie, Westfälische Wilhelms-Universität Münster, Schlossplatz 7, D 48149 Münster

Uwe Stege and Robert Schöllhorn

Institut für Allgemeine und Anorganische Chemie, Technische Universität Berlin, Strasse des 17, Juni 135, D10623 Berlin

Received March 31, 1998. Revised Manuscript Received August 10, 1998

The structures of the ternary Chevrel phases $CdMo_6Se_8$ and $Cd_2Mo_6Se_8$ have been studied by several complementary ^{111}Cd NMR spectroscopic techniques. Specifically, cadmium mobility and bonding properties are probed by temperature and frequency dependent measurements of static line shapes, magic angle spinning (MAS) NMR spectra, and spin−lattice relaxation rates. Furthermore, models for the spatial cadmium distribution are tested on the basis of $^{111}Cd-^{111}Cd$ dipole−dipole interactions, measured by spin−echo decay spectroscopy on isotopically labeled materials (97% ^{111}Cd). $CdMo_6Se_8$ undergoes a phase transition near 130 K; the cadmium ions are static on the NMR time scale over the whole temperature range in both phases. The spatial cation distribution is close to homogeneous, and it specifically excludes the presence of Cd−Cd dimers. For the high-temperature phase, the ^{111}Cd spectra indicate a large degree of static disorder. In addition, the large ^{111}Cd chemical shift temperature coefficient and fast spin−lattice relaxation reveal strong interactions between the intercalated cadmium atoms and the conduction band wave functions of the Mo_6Se_8 matrix. This behavior is typical for charge-transfer intercalation compounds in which the conduction band is only partially filled. $Cd_2Mo_6Se_8$, which crystallizes in the rhombohedral $R\bar{3}$ structure, shows the typical NMR signature of a rigid, semiconducting compound. The intercalated metal species show no apparent interaction with conduction electron wave functions. ^{111}Cd MAS and spin−echo decay data suggest a disordered atomic distribution of Cd^{2+} ions with a minimum Cd−Cd internuclear distance of 258 pm.

Introduction

Ternary molybdenum cluster chalcogenides of stoichiometry $A_xMo_6X_8$ (A = main group or transition metal, X = S, Se) have attracted considerable interest because of their remarkable physical and electronic properties. Compounds in which A = Sn or Pb are high-temperature superconductors with high critical magnetic field strengths.[1] Furthermore, electrochemical intercalation of the parent binary phase Mo_6S_8 with monovalent cations such as lithium and copper results in fast ionic conducting materials suitable for battery cathode applications.[2]

The overwhelming majority of the Chevrel phases crystallize in the rhombohedral space group $R\bar{3}$.[3] The basic structure is shown in Figure 1. It can be described as a three-dimensional arrangement of Mo_6X_8 units which themselves consist of X_8 cubes that surround the Mo_6 octahedra. The vacant sites form a three-dimensional system of interconnected channels that can be occupied by the metal atoms A. With respect to these occupancies, two situations can be differentiated: Due to size constraints, large cations with radii above a critical value of 100 pm tend to occupy the central 8-coordinated position, limiting the stoichiometry of these phases to AMo_6X_8. In contrast, smaller cations are disordered over 12 potential lattice positions around the unit cell origin, having distorted tetrahedral chalcogen environments. These sites are distributed on two different rings—an inner and an outer ring—each one of which consists of six equivalent positions.[1,3,4] The occupancies of these ring positions and their dependences on metal cation content have been subject to many structural investigations.

A variety of Chevrel phases also crystallize in the triclinic space group $P\bar{1}$. In this structure the metal ions are surrounded by four chalcogen atoms in a distorted tetrahedron and are arranged in the form of A···A pairs. Several Chevrel compounds display polymorphism, $R\bar{3}$ being the high- and $P\bar{1}$ the low-temperature phase.[1,3,4]

(1) Fischer, O.; Maple, M. B. *Top. Curr. Phys.* **1982**, 32.
(2) Schöllhorn, R. *Angew. Chem., Int. Ed. Engl.* **1980**, *19*, 983.
(3) Yvon, K. *Current Topics Materials Science;* North-Holland (Amsterdam, 1979; Vol. 3, p 53.
(4) Prigge, C.; Müller-Warmuth, W.; Gocke, E.; Schöllhorn, R. *Solid State Ionics* **1993**, *62*, 143

10.1021/cm9802043 CCC: $15.00
Published on Web 10/02/1998

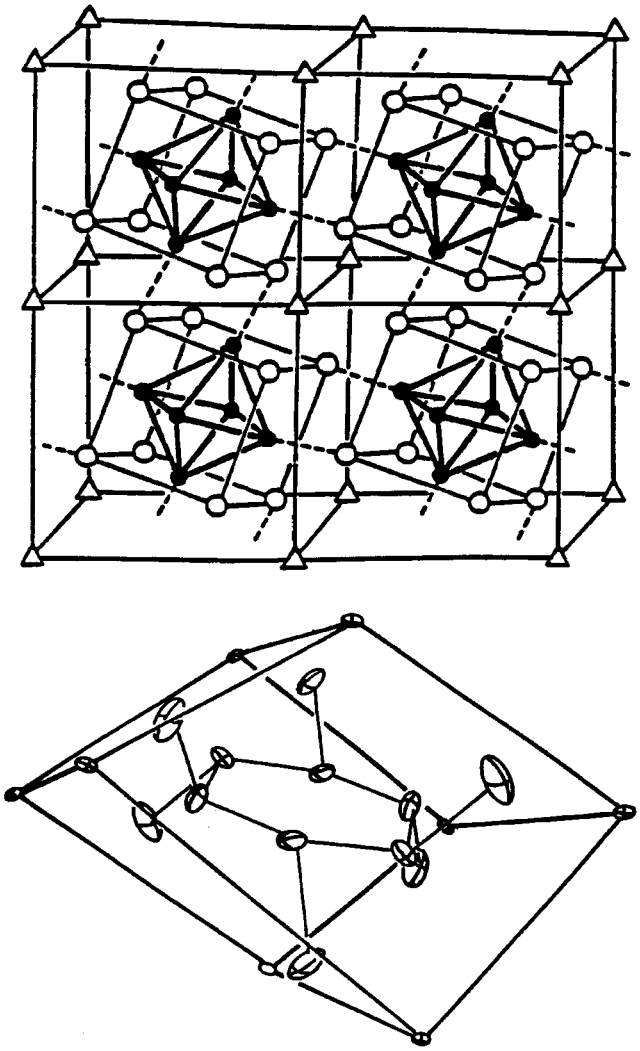

Figure 1. Crystal structure scheme of Chevrel phases A_x-Mo_6X_8 (X = S,Se) (from refs 1 and 3). (top) Arrangement of the Mo_6X_8 framework: open circles, X; closed circles, Mo; triangles, vacancies occupied by large A cations. (bottom) Disordered sites occupied by small A cations: on-edge eight X atoms belonging to different X_8 cubes; interior and exterior hexagon rings of the vacant distorted tetrahedral sites.

According to band structure calculations, the maximum possible charge-transfer amounts to four electrons per Mo_6 cluster, limiting the intercalation to four monovalent or two divalent cations per host formula unit.[5] However, this limit can only be reached with small cations. At low intercalation levels, phases are formed with complete charge transfer, leaving single cations in one of the potential sites of a cavity. At higher intercalation levels, the charge transfer is no longer complete and the partial occupation of the upper band with electrons from the intercalated metal species results in superconducting and metallic materials. At the maximum intercalation levels, complete occupation of the upper band with the four electrons required results in a metal/semiconductor transition. These predictions are generally borne out by nuclear magnetic resonance (NMR) chemical shift measurements of various intercalated metal species. For example, the ^{7}Li nuclei show large Knight shifts in the phases $Li_3Mo_6S_8$ and $Li_3Mo_6Se_8$, and likewise in the $Li_{3.8}Mo_6X_8$ phases. In contrast, near-zero values are observed for both Li_1-Mo_6S_8 and $Li_4Mo_6S_8$.[6−8]

The present contribution deals with the site distribution and electronic properties in cadmium-intercalated Chevrel phases. Since Cd^{2+} possesses an ionic radius (97 pm) very close to the critical value, the intercalation behavior observed is critically dependent on host lattice dimensions. Thus, the intercalation stoichiometry is limited to $x = 1$ in Mo_6S_8, whereas in Mo_6Se_8, where the vacancy sites are slightly larger, two cadmium ions per formula unit can be intercalated.[9] Two distinct line phases, $CdMo_6Se_8$ and $Cd_2Mo_6Se_8$, have been identified, and their lattice dimensions have been characterized by X-ray powder diffractometry. However, due to the lack of single-crystal X-ray data, the distribution of the cadmium ions over these sites is unknown. Likewise, the electronic properties of these materials have not been characterized to date. The experimental observation that the related compound $Zn_2Mo_6S_8$ is superconducting[10] has led to speculations that charge transfer in this compound is incomplete, and better described by the scheme $(Zn-Zn)^{4\delta+}[Mo_6S_8]^{4\delta-}$ ($\delta < 1$), rather than $(Zn^{2+})_2[Mo_6S_8]^{4-}$. Similar models are conceivable for the cadmium homologue. Models based on partial charge transfer are also invoked for explaining the unexpectedly high mobility of divalent cations as recently detected in $Ni_2Mo_6S_8$ by neutron diffraction[11] and in Cu^{2+}-doped $HgMo_6S_8$ by EPR spectroscopy.[12] Confirmation of such high mobility for other divalent cations (such as Cd^{2+}) and by independent experimental methods would be highly desirable.

Solid-state nuclear magnetic resonance offers a variety of experimental strategies to address such questions. High-resolution NMR studies using magic angle spinning (MAS) have the potential to reveal site multiplicities for the testing of various order/disorder models. A parameter quite sensitive toward the spatial distribution of the cations is the strength of the magnetic dipole−dipole interactions among the intercalated nuclei.[13] These dipolar couplings can be measured selectively by spin−echo decay spectroscopy.[14,15] In particular, the short internuclear distance associated with a postulated $[Cd-Cd]^{2+}$ dimer would become clearly evident in such measurements. Guest−host lattice charge transfer can be assessed on the basis of NMR chemical shift and relaxation time measurements, as previously shown for many other intercalation compounds.[16] Finally, variable temperature static NMR

(5) Hughbanks, T.; Hoffmann, R. *J. Am. Chem. Soc.* **1983**, *105*, 1150.

(6) Aselmann, G.; Müller-Warmuth, W.; Gocke, E.; Schöllhorn, R. *Z. Phys. Chem.* **1987**, *151*, 103.

(7) Gocke, E.; Schöllhorn, R.; Aselmann, G.; Müller-Warmuth, W. *Inorg. Chem.* **1987**, *26*, 1805.

(8) Prigge, C.; Müller-Warmuth, W.; Gocke, E.; Schöllhorn, R. *Chem. Mater.* **1993**, *5*, 1493.

(9) Gocke, E.; Schramm, W.; Dolscheid, P.; Schöllhorn, R. *J. Solid State Chem.* **1987**, *70*, 71.

(10) Schramm, W. Dissertation, University of Münster, 1981.

(11) Ritter, C.; Nöldeke; C.; Press: W.; Stege, U.; Schöllhorn, R. *Z. Phys. B.* **1993**, *92*, 437.

(12) Kadam, R. M.; Sastry, M. D.; Iyer, R. M.; Gopalakrishnan, I. K.; Yakhmi, J. V. *J. Phys. Condens. Matter* **1997**, *9*, 551.

(13) Van Vleck, J. H. *Phys. Rev.* **1948**, *74*, 1168.

(14) Engelsberg, M., Norberg, R. E. *Phys. Rev.* **1972**, *B5*, 3395.

(15) Boden, N.; Gibb, M.; Levine, Y. K.; Mortimer, M. *J. Magn. Reson.* **1974**, *16*, 471.

(16) Müller-Warmuth, W. *Progress in Intercalation Research (Review);* Müller-Warmuth, W., Schöllhorn, R., Eds.; Klüwer: Boston, 1994; p 339.

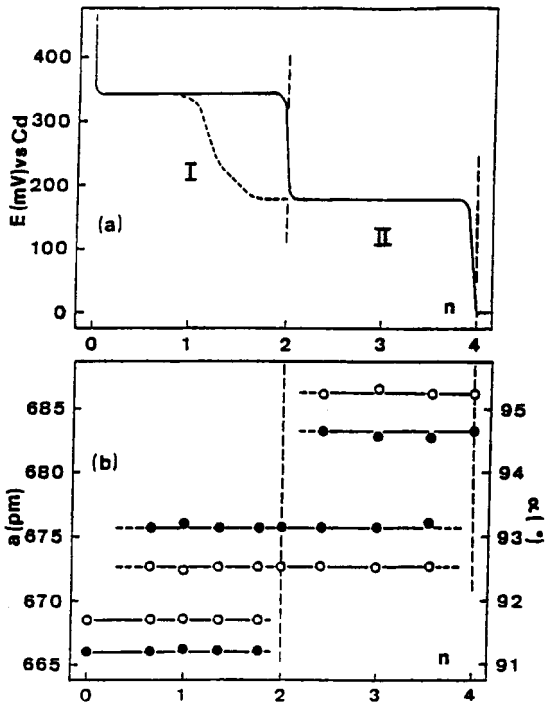

Figure 2. Intercalation of Cd^{2+} into Mo_6Se_8: (a) Plot of voltage vs *n*, the amount of charge transferred per formula unit. Dashed curve, first electrochemical intercalation; solid curve, electrochemical intercalation after repeated cycling. (b) Evolution of lattice parameters *a* (closed circles) and α (open circles) as a function of *n*, the number of charges transferred per unit of Mo_6Se_8: bottom traces, lattice parameters observed for Mo_6Se_8; middle traces, lattice parameters observed for $CdMo_6Se_8$; top traces, lattice parameters observed for $Cd_2Mo_6Se_8$.

Table 1. Crystal Lattice Parameters of $CdMo_6Se_8$ and $Cd_2Mo_6Se_8$

	a_R (pm)	α (deg)
$CdMo_6Se_8$	675.7	92.53
$Cd_2Mo_6Se_8$	683.2	95.25

line shape and spin−lattice relaxation time data are able to provide important information on the atomic mobility of the intercalated species. With these goals in mind, we present here a comprehensive structural NMR characterization of the phases $CdMo_6Se_8$ and $Cd_2Mo_6Se_8$.

Experimental Section

Sample Preparation and Characterization. Mo_6Se_8 was prepared from the ternary compound $Cu_2Mo_6Se_8$, as previously described.[17] Intercalation of cadmium was effected via cathodic reduction in a galvanic cell $Cd/CdSO_4$ (2 M), H_2O/Mo_6Se_8. Additional details of the preparation procedure can be found in ref 9. Figure 2 shows the voltage/charge transfer diagram obtained relative to metallic cadmium. Typical two-phase behavior is observed, corresponding to the formation of two separate compounds with the stoichiometries $CdMo_6Se_8$ and $Cd_2Mo_6Se_8$, respectively. Table 1 summarizes the crystallographic lattice parameters measured by powder diffractometry, indicating that cadmium intercalation has a considerable effect on the lattice dimensions.

For each of the two stoichiometries, two samples were prepared, corresponding to the natural isotopic distribution and 97% enrichment with ^{111}Cd, respectively.

NMR Studies. Static variable temperature (110−300 K) ^{111}Cd solid-state NMR experiments were carried out at 63.633 MHz, using a Bruker CXP-300 spectrometer equipped with a multinuclear probe and a TECMAG data acquisition system. A solid echo technique $90°_x-\tau-90°_y$ (τ =10−20 μs) was used to avoid signal distortions due to probe ringing and delayed receiver recovery. Spin−lattice relaxation times were measured by the saturation recovery technique, while spin−spin relaxation times related to homonuclear $^{111}Cd-^{111}Cd$ dipole−dipole couplings were determined by the $90°-t_1-180°$ (Hahn spin−echo) sequence. To avoid experimental artifacts due to tuning and amplifier instabilities, the t_1 values were incremented in a random order. In all of these experiments, the 90° pulse lengths ranged between 8 and 10.5 μs. High-resolution MAS-NMR data were obtained at 106.1 MHz on a Bruker AVANCE 500 MHz spectrometer, using a 4 mm MAS NMR probe, operating at a spinning speed of 6.0 kHz. These spectra were obtained using short pulses of 3 μs length. Chemical shifts are reported with a 3 M $CdSO_4$ solution as external reference.

Results and Data Analysis

Variable Temperature ^{111}Cd NMR of $CdMo_6Se_8$. Figure 3a summarizes the variable temperature static spectra of $CdMo_6Se_8$. For reasons of improved signal-to-noise ratio, results are shown for the isotopically enriched compound; however, identical results were obtained on corresponding samples with natural isotopic distribution. The phase transition near 130 K is clearly evident in the spectra. The line shapes observed for the low-temperature phase reflect an approximately axially symmetric chemical shift tensor; corresponding principal values are listed in Table 2. The phase transition near 130 K is reflected by a dramatic change of the isotropic chemical shift by approximately 300 ppm, accompanied by a pronounced line shape change. It becomes totally impossible to fit the spectra observed above 130 K to a unique set of chemical shift tensor components. As the temperature is increased, the center of gravity is shifted linearly to higher frequency, whereas only slight changes in the line shapes are evident. To address the question whether the most unusual static line shapes are the result of static or dynamic disordering, additional holeburning experiments,[18] magic angle spinning studies, and spin−lattice relaxation measurements were conducted as a function of temperature and field strength. In the holeburning experiments, it was found to be possible to invert an arbitrarily chosen narrow spectral region of the static line shape by a DANTE sequence.[19] This experiment demonstrates that the line shape is dominated by inhomogeneous, rather than homogeneous, broadening.

The MAS NMR spectra are shown in Figure 3b. As in the static spectra, the pronounced temperature dependence of the isotropic chemical shift is evident. Within the temperature region 150 K ≤ *T* ≤ 300 K, the shift increases linearly from 414 to 650 ppm. Furthermore, there is no distinction of individual cadmium sites, and surprisingly large line widths are observed. These are found to be temperature-independent over the entire temperature range considered: room-temperature MAS spectra obtained at 7.0 and 11.7 T indicate a

(17) Fischer, C.; Gocke E.; Stege, U.; Schöllhorn, R. *J. Solid State Chem.* **1993**, *102*, 54.

(18) Reimer, J. A.; Vaughan, R. W.; Knights, J. C. *Phys. Rev. B* **1981**, *24*, 3360.

(19) Bodenhausen, G.; Freeman, R.; Morris, G. A. *J. Magn. Reson.* **1976**, *23*, 171.

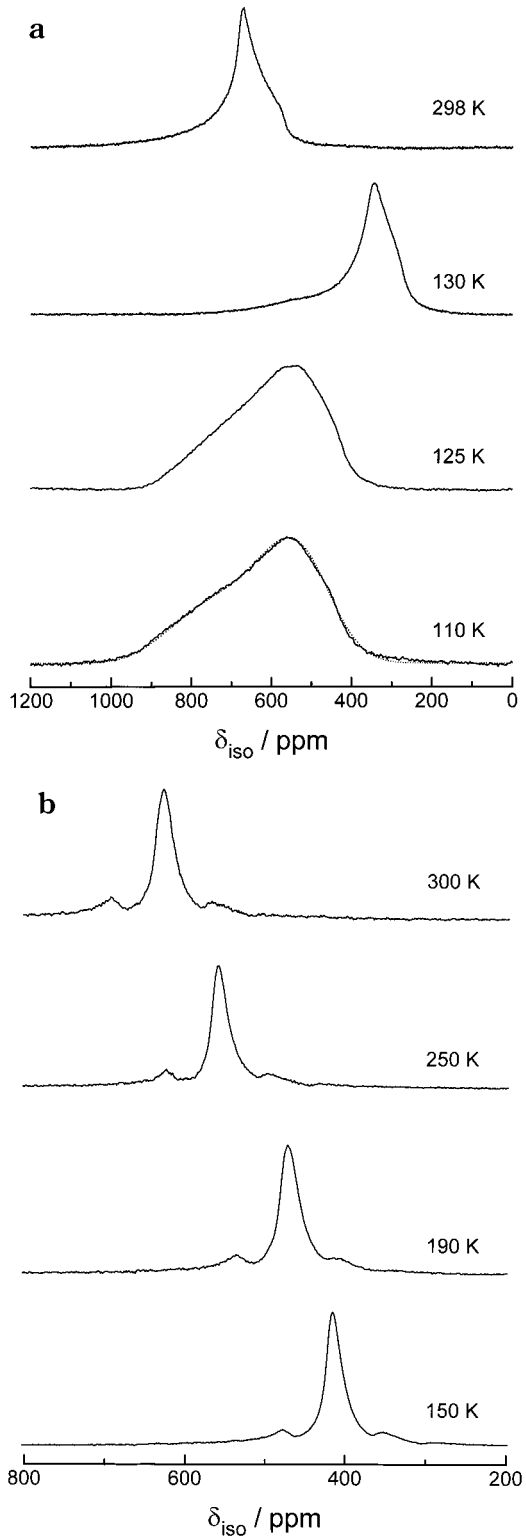

Figure 3. Variable temperature ^{111}Cd NMR spectra of $CdMo_6Se_8$: (a) static spectra at 63.63 MHz. A theoretical fit of the 110 K line shape is included (dotted curve). (b) MAS NMR spectra at 106.1 MHz.

constant line width of ca. 21 ppm, suggesting that the shape of the NMR spectra is dominated by a distribution of isotropic chemical shifts.

Figure 4 summarizes the spin−lattice relaxation data. The spin−lattice relaxation times are extremely short (on the order of 1−10 ms). The rates increase linearly with temperature but are independent of Larmor frequency. Additional detailed inversion recovery experiments indicate the absence of detectable T_1-anisotropy.

Variable Temperature ^{111}Cd NMR of $Cd_2Mo_6Se_8$. Results on $Cd_2Mo_6Se_8$ are summarized in Figure 5. Despite the target composition $Cd_2Mo_6Se_8$, this sample was found to contain an admixture of $CdMo_6Se_8$, resulting in spectral overlap at certain temperatures. The line shape and line position of $Cd_2Mo_6Se_8$ is almost independent of temperature and reflects the approximately axial symmetry of the ^{111}Cd shielding tensor. The room temperature MAS NMR spectrum of $Cd_2Mo_6Se_8$ reveals a single broad resonance at 560 ppm (line width 22 ppm), indicating disorder in the cation sublattice. The spin−lattice relaxation times are on the order of several minutes, as typically observed for other semiconducting Cd compounds.

^{111}Cd Spin−Echo Decay Spectroscopy. As discussed previously,[14,15,18] homodipolar interactions among spin = $^1/_2$ nuclei can be evaluated selectively by measuring the normalized spin−echo intensity I/I_o following a $90°-t_1-180°-t_1$ pulse sequence as a function of evolution time $2t_1$. For systems of many interacting spins, a Gaussian decay function is expected,

$$I(2t_1)/I_o = \exp -[(2t_1)^2 M_{2d}/2] \qquad (1)$$

yielding the dipolar second moment M_{2d}.

Such experimental values can be compared with theoretical values calculated from internuclear distances r_{ij} using van Vleck theory:[13]

$$M_{2d} = (4/15)(\mu_o/4\pi)^2 I(I+1)\gamma^4\hbar^2 \sum_{i\neq j} r_{ij}^{-6} \qquad (2)$$

In this equation, μ_o is the magnetic permeability constant, while I and γ are the spin quantum number and gyromagnetic ratio of the nuclei studied. This approach is rigorously applicable only if the differences between the resonance frequencies of neighboring spins are larger than the frequency characterizing the strength of their dipole−dipole coupling, thus eliminating the contributions of flip-flop transitions to the second moment. The numerical prefactor $^4/_{15}$ accounts for this assumption. If the latter condition is not fulfilled, apparently higher experimental M_{2d} values are measured; however, the theory is only approximately applicable under these conditions.[20] Comparison of the static spectra with the spin−echo decay data illustrates that in both $CdMo_6Se_8$ and $Cd_2Mo_6Se_8$ inhomogeneous broadening due to chemical shift anisotropy and distribution is dominant, hence justifying the use of eq 2 for analyzing the spin−echo decays.

The opportunity of analyzing the spatial Cd spin distribution in these intercalation compounds on the basis of homodipolar ^{111}Cd−^{111}Cd interactions provided the major impetus for the preparation of isotopically labeled samples in this study. Figure 6 shows the spin−echo decay data of the isotopically enriched $CdMo_6Se_8$ material at various temperatures. At room temperature, an exponential decay is observed, yielding an apparent spin−spin relaxation time of 1.7 ms. This rather rapid decay is essentially controlled by spin−

(20) Lathrop, D.; Franke, D.; Maxwell, R. Tepe, T.; Flesher, R.; Zhang, Z.; Eckert, H. *Solid State Nucl. Magn. Reson.* **1992**, *1*, 73.

Table 2. Chemical Shift Parameters and Dipolar Second Moments $M_2(^{111}Cd-^{111}Cd)$ in $CdMo_6Se_8$ and $Cd_2Mo_6Se_8$ at Different Temperatures

temp, K	space group	δ_{11} (±10 ppm)	δ_{22} (±10 ppm)	δ_{33} (±10 ppm)	δ_{iso} (±1 ppm)	Δ^c (±100 Hz)	$M_2/10^6$ s^{-2} (±10%)
				$CdMo_6Se_8$			
298	$R\bar{3}$	*a*	*a*	*a*	650	*a*	*a*
150	$R\bar{3}$	*a*	*a*	*a*	415	*a*	0.037
110	unknown	544	544	787	625	4900	0.088
				$Cd_2Mo_6Se_8$			
298	$R\bar{3}$	555	555	600	560	450	0.79
110	$R\bar{3}$	576	576	623	592±10[b]	600	*a*

[a] Not determined (see the text). [b] From static NMR. [c] Convolution parameter for simulation of the static line shape, comprising dipolar broadening and distribution effects of chemical shift parameters.

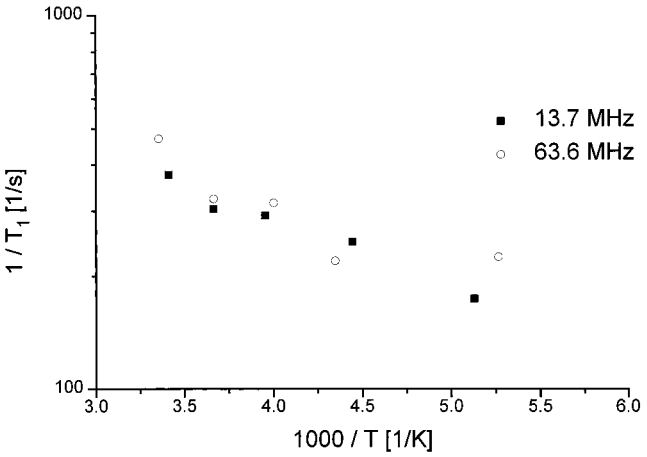

Figure 4. ^{111}Cd nuclear spin lattice relaxation rates of $CdMo_6Se_8$ as a function of temperature and resonance frequency.

lattice relaxation. At lower temperatures near the phase transition, approximate Gaussian behavior is observed. The fit to the data can be improved, however, by taking into account that even at temperatures this low, spin−lattice relaxation is extremely fast in this compound and thus makes a substantial contribution to the spin−echo decay. Therefore, eq 1 must be replaced by

$$I(2t_1)/I_o = \exp -[(2t_1)^2 M_{2d}/2] \exp -(2t_1/T_1) \quad (3)$$

Using $T_1 = 6.6$ ms, measured by the saturation recovery technique, a value $M_{2d} = (0.037 \pm 0.004) \times 10^6$ s^{-2} is obtained for the high-temperature phase at 150 K. Using $T_1 = 10.6$ ms, a value $M_{2d} = (0.088 \pm 0.008) \times 10^6$ s^{-2} is obtained for the low-temperature phase at 110 K. Figure 7 shows the corresponding data for isotopically enriched $Cd_2Mo_6Se_8$ at room temperature. In this case, a minor complication in the analysis arises from the fact that the sample is not entirely phase pure. Rather, the ^{111}Cd spin−echo signal contains a 20% contribution from $CdMo_6Se_8$, whose spin−echo behavior is superimposed on that of the target compound. A satisfactory fit to the experimental data can be obtained according to

$$I(2t_1)/I_o = 0.2 \exp -(2t_1/T_2) + 0.8 \exp -[(2t_1)^2 M_{2d}/2] \quad (4)$$

Inserting the apparent room-temperature T_2 value of the $CdMo_6Se_8$ admixture (1.7 ms), the analysis yields $M_{2d} = (0.79 \pm 0.08) \times 10^6$ s^{-2} for $Cd_2Mo_6Se_8$.

Discussion

Structure and Bonding in $CdMo_6Se_8$. The exact crystal structure of the low-temperature modification of $CdMo_6Se_8$, which is stable at temperatures below 130 K, is not known, although analogy with several other Chevrel phases suggests that the triclinic phase is formed. While the lack of definite structural information precludes a detailed discussion of the spectroscopic parameters observed, various conclusions can be drawn on the basis of the ^{111}Cd NMR data reported here. The static powder spectrum reveals approximately axially symmetric chemical shielding. The line shape is rather poorly defined, however, suggesting that the Cd^{2+} atoms may be distributed over several slightly different sites. The dipolar second moment (0.088×10^6 s^{-2}) can be compared to a variety of structural scenarios. On one hand, the data clearly rule out the occurrence of Cd_2^{2+} ions. A typical Cd−Cd internuclear distance for such a species is 256 pm, as observed experimentally in $Cd_2(AlCl_4)_2$.[21] Comparable distances have been found for the metal ions in $Fe_2Mo_6S_8$ (251 pm),[22] $Cu_{1.8}Mo_6S_8$ (258 pm),[23] and $Ni_{0.66}Mo_6Se_8$ (226 pm).[24] In $CdMo_6Se_8$, only 50% of the dimeric cation sites present in the triclinic structure can be occupied. Four possible scenarios are (a) preferred dimer formation (as in $Ni_{0.66}Mo_6Se_8$), (b) random distribution with statistical formation of dimers, (c) ordered distributions with complete exclusion of dimers, and (d) disordered distributions with complete exclusion of dimers. From eq 2 the corresponding theoretical second moments can be calculated for these scenarios.

The individual contribution of a spin pair at a distance of 256 pm to the dipolar second moment is 0.83×10^6 s^{-2}, i.e., 10 times larger than observed experimentally. On the basis of this discrepancy, scenario a can be ruled out. In scenario b, 50% of the Cd ions are predicted to occur within dimers. This model predicts that the ^{111}Cd spin−echo decay should have a pronounced bimodal character, in contrast to experimental observation. The closest approach to the ordering model (c) would be a homogeneous Cd distribution in space. This scenario, in which the Cd ions adopt the maximum possible internuclear distances from each other, results in a second moment value of 0.020×10^6 s^{-2}, which is much lower than determined experimentally. Finally, in scenario d, the A positions of the triclinic structure are occupied randomly, while the formation of dimers is excluded. On the basis of the known atomic positions

(21) Staffel, T.; Meyer, G. *Z. Anorg. Allg. Chem.* **1987**, *548*, 45
(22) Yvon, K.; Chevrel, R.; Sergent, M. *Acta Crystallogr.* **1980**, *B36*, 685.
(23) Yvon, K.; Bailiff, R.; Flükiger, R. *Acta Crystallogr.* **1979**, *B35*, 2859. Yvon, K.; Paoli, A.; Flükiger, R.; Chevrel, R. *Acta Crystallogr.* **1977**, *B33*, 3066.
(24) Bars, O.; Guillevic, Grandjean, D.; J. Solid State Chem. **1973**, *6*, 335.

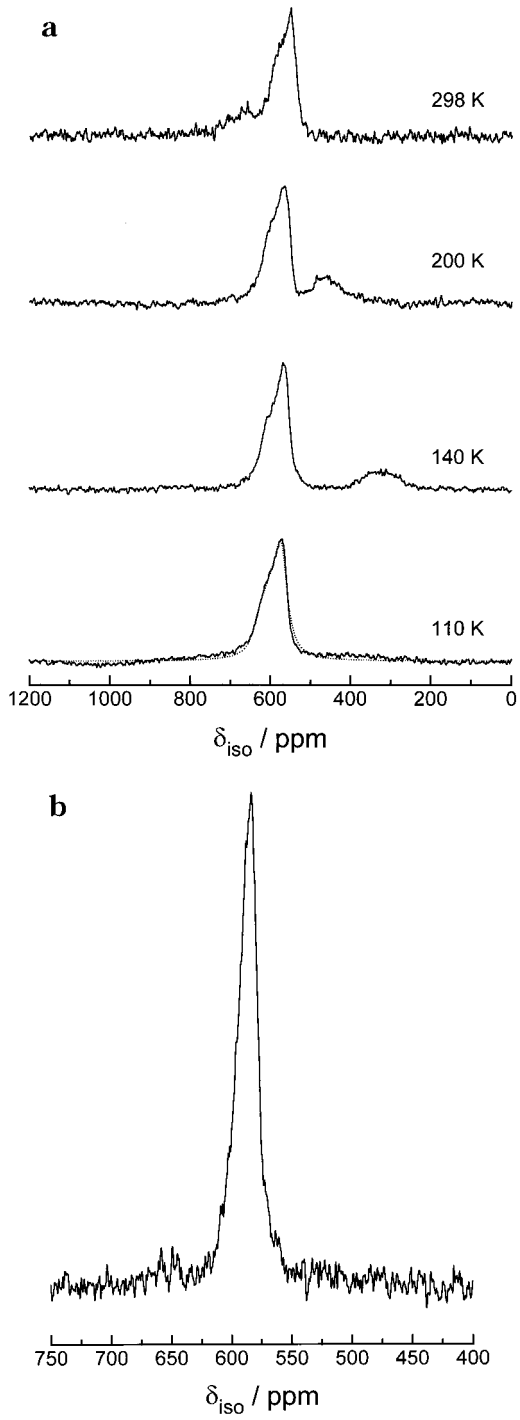

Figure 5. ^{111}Cd NMR spectra of $Cd_2Mo_6Se_8$: (a) variable temperature static spectra at 63.63 MHz. A theoretical fit of the 110 K line shape is included (dotted curve). The broad minority peak seen in each spectrum belongs to an impurity of $CdMo_6Se_8$. (b) Room temperature MAS NMR spectrum at 106.1 MHz.

in triclinic $Cu_{1.8}Mo_6S_8$, we can calculate for scenario d a dipolar second moment of 0.057×10^6 s^{-2}, which comes closest to the experimental value. Thus, we conclude that scenario d represents the best approximation for the spatial cation distribution in the low-temperature form of $CdMo_6Se_8$.

The spectroscopic features that are most striking for the high-temperature R$\bar{3}$ phase are the unusual static ^{111}Cd NMR line shape, the short spin−lattice relaxation time, and the strong temperature dependence of the

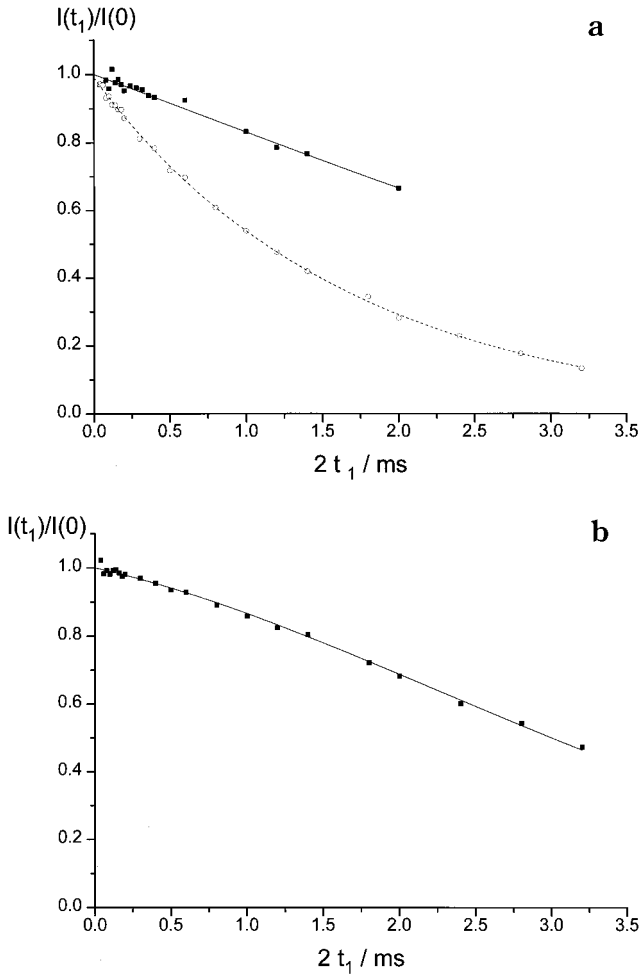

Figure 6. ^{111}Cd spin−echo decay spectroscopy of $CdMo_6Se_8$: (a) R$\bar{3}$ structure: room-temperature data (open circles) and 150 K data (solid squares). The solid curve corresponds to a theoretical fit to eq 3; see the text. (b) Low-temperature structure (110 K). The solid curve corresponds to a theoretical fit to eq 3; see the text.

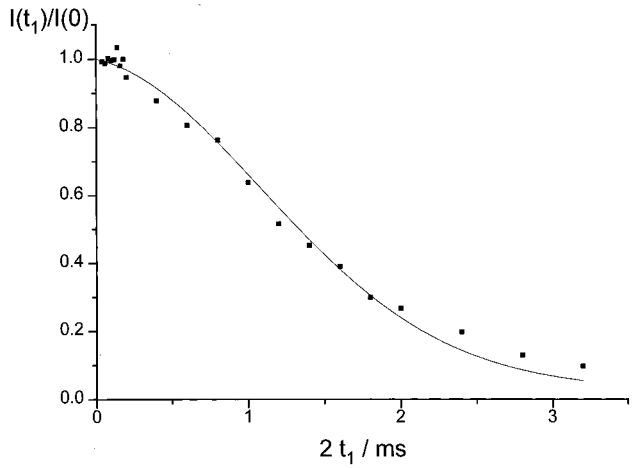

Figure 7. Room temperature ^{111}Cd spin−echo decay spectroscopy of $Cd_2Mo_6Se_8$. The solid curve corresponds to a fit to eq 4.

resonance frequency. In principle, such line shapes could arise from an anisotropically restricted motion, resulting in only partial averaging of the chemical shift anisotropy. However, none of the temperature- and field-dependent NMR experiments discussed above give

any indications for dynamic phenomena on the NMR time scale. If motion were present, one would have expected temperature-dependent changes in the MAS NMR line width and a frequency-dependent contribution to the spin−lattice relaxation rate, unless this motion is fast on the NMR time scale down to the phase transition temperature at 130 K. Since the latter appears rather unlikely, we conclude that the spectra of $CdMo_6Se_8$ are dominated by static disorder. The line shape can be accounted for by assuming that two of the three principal components of the chemical shift tensor are quite well-defined, whereas the third one (σ_{33}) is subject to a wide distribution.

The broad MAS NMR line observed allows no conclusions about possible occupancies of inner- and outer-ring sites. Still, the observation of a single, (albeit broad) MAS peak is consistent with the exclusive occupancy of the inner-ring positions, as observed in most Chevrel phases $A_xMo_6X_8$ (small A cations), where x lies in the vicinity of 1. Again, both the static NMR line shape and the large MAS NMR line width suggest that the Cd environments in the high-temperature phase are characterized by a continuous range of local distortions. The small value of M_2 ($^{111}Cd-^{111}Cd$) indicates that the cadmium distribution is close to uniform.

The resonance shifts in $CdMo_6Se_8$ are substantially smaller than for Cd metal (3421 ppm),[25] and the experimental product $T_1\delta^2$ is not proportional to T^{-1}, as expected for an ordinary metal according to the Korringa equation.[26] Nevertheless, the temperature-dependent spectra reveal a distinct isotropic paramagnetic contribution to the resonance shift which is typical of a scalar interaction of the ^{111}Cd spins with unpaired conduction electron density at the Fermi edge. This conclusion is further supported by the large, frequency-independent spin−lattice relaxation rates. The increase of both the isotropic shift component and the relaxation rates with temperature indicates a strong temperature-dependent interaction between cadmium and conduction electron wave functions. This behavior has been seen previously for the intercalant metal resonances of the Chevrel phase $Li_{3.0}Mo_6Se_8$[8] and of other intercalation compounds as well.[27−29] This strong temperature dependence appears to be a common feature of many intercalation compounds in which the host lattice conduction band is incompletely filled.

Structure and Bonding in $Cd_2Mo_6Se_8$. Contrary to the situation in the $CdMo_6Se_8$ phase, the chemical shift in $Cd_2Mo_6Se_8$ is only weakly temperature-dependent and the spin−lattice relaxation times are very long. Both the static powder pattern and the broad MAS NMR resonance line indicate considerable disorder in the cadmium distribution in this phase as well, and no definite conclusions about site occupancies are possible. The spin−echo decay data, shown in Figure 7, offer independent experimental criteria for the development of realistic atomic distribution models. Since the precise atomic positions of the cadmium ions in $Cd_2Mo_6Se_8$ are not known, due to lack of single-crystal X-ray data, the $Cu_2Mo_6Se_8$ structure is taken as a model. In this compound, the two opposing ends of the inner-ring positions are at a distance of 230 pm. Filling the inner-ring sites of $Cd_2Mo_6Se_8$ in this manner, an overall M_{2d} value of 1.57×10^6 s^{-2} is calculated, which is considerably larger than the experimental value of 0.79×10^6 s^{-2}. Thus, one may conclude that the Cd^{2+} ions are most likely distributed over inner- and outer-ring positions, unless the inner-ring dimensions in $Cd_2Mo_6Se_8$ are considerably different from those in $Cu_2Mo_6Se_8$. From the experimental second moment of 0.79×10^6 s^{-2}, we can conclude that the minimum Cd−Cd distance is 258 pm.

Conclusions

In summary, these results indicate that NMR can provide detailed qualitative information on the structure, bonding, and dynamics of Chevrel intercalation compounds with unknown crystal structures. Unlike the divalent cations present in $Ni_2Mo_6S_8$ and Cu^{2+}-doped $HgMo_6S_8$, the Cd^{2+} ions appear to be rigid on the NMR time scale in both $CdMo_6Se_8$ and $Cd_2Mo_6Se_8$.

A review of the electronic properties of the intercalation compounds of various different host matrices (e.g. Chevrel phases, graphite, C_{60}) reveals a rather universal behavior as a function of the intercalation level. Compounds corresponding to the maximum intercalation level possess a completely filled conduction band. Here, charge transfer from the metal to the conduction band is essentially complete, and the compound exhibits classical semiconducting behavior. Typical examples for such behavior are LiC_6, Rb_6C_{60}, $Li_4Mo_6S_8$, and (from the present study) $Cd_2Mo_6Se_8$. In contrast, intercalation compounds in which the host matrix conduction band is only partially filled frequently exhibit metallic behavior and may become superconducting at low temperatures. The NMR spectra of these compounds are generally characterized by a large temperature dependence of the chemical shift and extremely fast spin−lattice relaxation. These data indicate that charge transfer from the metal atom to the host lattice conduction band is incomplete in such compounds and that there is a strong interaction between the metal atom and the conduction band wave functions. Typical examples for such behavior are CsC_{12}, Rb_3C_{60}, $Li_3Mo_6S_8$, and (from the present study) $CdMo_6Se_8$. The spin−echo decay data for $CdMo_6Se_8$ indicate, however, that the mechanism by which charge density is localized on the cadmium ion in this compound does not involve the formation of $(Cd-Cd)^{4\delta+}$ dimers. This situation differs from that in $Li_3Mo_6Se_8$, where clustering of the Li^+ ions has been inferred from the NMR data.[8] In $Cd_2Mo_6Se_8$, the $^{111}Cd-^{111}Cd$ dipole−dipole interactions are considerably stronger than in $CdMo_6Se_8$. A good fit to the experimental spin−echo decay can be obtained by assuming that the two Cd^{2+} ions occupy disordered positions of the inner and outer rings of cation sites in the structure, analogously to the situation in $Cu_2Mo_6Se_8$. The minimum $Cd^{2+}-Cd^{2+}$ distance is estimated as 258 pm.

(25) Andrew, E. R.; Hinshaw, W. S.; Tiffen, R. S. *J. Magn. Reson.* **1974**, *15*, 191.
(26) Slichter, C. P. *Principles of Magnetic Resonance*; Springer-Verlag: Berlin, 1978; p 149.
(27) Eckert, H.; Müller-Warmuth, W.; Schramm, W.; Schöllhorn, R. *Solid State Ionics* **1984**, *12*, 1.
(28) Estrade-Swarckopf, C., J.; Lauginie, P.; van der Klink, J.; G., D.; Lagrange, P., In *Physics of Intercalation Compounds*; Pietronero, L.; Tosatti, E., Eds., Proc. Int. Conf. 1981; Springer-Verlag: Berlin, 1981; p 274.
(29) Zimmer, G.; Helmle, M.; Mehring, M.; Rachdi, F.; Reichenbach, J.; Firlej, L.; Bernier, P. *Europhys. Lett.* **1993**, *24*, 59.

Acknowledgment. Financial support by the Wissenschaftsministerium Nordrhein-Westfalen and by the Fond der chemischen Industrie is gratefully acknowledged. We thank Dr. Johannes Janssen (now with Deutsche Forschungsgemeinschaft, Bonn) for his participation in the initial stages of this work.

CM9802043